



Published in final edited form as:

Immunity. 2015 October 20; 43(4): 803–816. doi:10.1016/j.immuni.2015.09.005.

Interleukin-4 Receptor α Signaling in Myeloid Cells Controls Collagen Fibril Assembly in Skin Repair

Johanna A. Knipper^{1,13}, Sebastian Willenborg^{1,13}, Jürgen Brinckmann², Wilhelm Bloch³, Tobias Maaß⁴, Raimund Wagener⁴, Thomas Krieg^{1,5,6}, Tara Sutherland⁷, Ariel Munitz⁸, Marc E. Rothenberg⁹, Anja Niehoff^{10,11}, Rebecca Richardson¹², Matthias Hammerschmidt^{5,6,12}, Judith E. Allen⁷, and Sabine A. Eming^{1,5,6,*}

¹Department of Dermatology, University of Cologne, 50937 Cologne, Germany

²Department of Dermatology and Institute of Virology and Cell Biology, University of Lübeck, 23562 Lübeck, Germany

³Department of Molecular and Cellular Sport Medicine, German Sport University Cologne, 50933 Cologne, Germany

⁴Department of Biochemistry, University of Cologne, 50937 Cologne, Germany

⁵Center for Molecular Medicine Cologne, University of Cologne, 50931 Cologne, Germany

⁶Cologne Excellence Cluster on Cellular Stress Responses in Aging-Associated Diseases, University of Cologne, 50674 Cologne, Germany

⁷Institute of Immunology and Infection Research, Centre for Immunity, Infection & Evolution, School of Biological Sciences, University of Edinburgh, EH9 3FL Edinburgh, UK

⁸Department of Clinical Microbiology and Immunology, The Sackler School of Medicine, The Tel-Aviv University, Ramat Aviv 69978, Israel

⁹Division of Allergy and Immunology, Cincinnati Children's Hospital Medical Center, University of Cincinnati College of Medicine, Cincinnati, OH 45229-3039, USA

¹⁰Institute of Biomechanics & Orthopedics, German Sport University Cologne, 50933 Cologne, Germany

¹¹Cologne Center for Musculoskeletal Biomechanics, University of Cologne, 50931 Cologne, Germany

¹²Institute of Developmental Biology, University of Cologne, 50674 Cologne, Germany

*Correspondence: sabine.eming@uni-koeln.de.

¹³Co-first author

SUPPLEMENTAL INFORMATION

Supplemental Information includes Supplemental Experimental Procedures, six figures, and three movies and can be found with this article online at <http://dx.doi.org/10.1016/j.immuni.2015.09.005>.

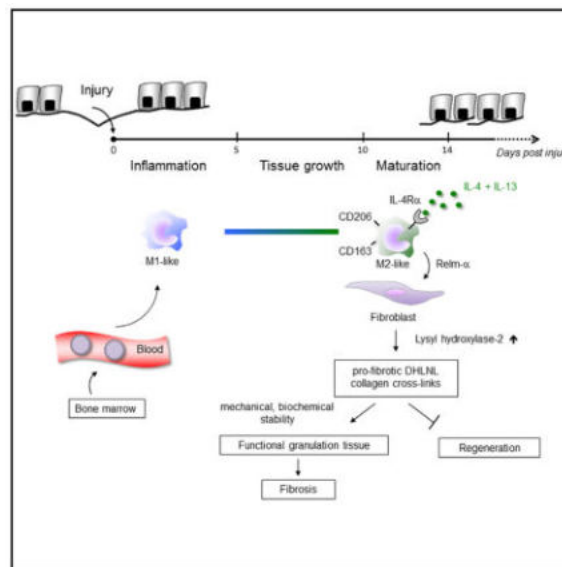
AUTHOR CONTRIBUTIONS

J.A.K., S.W., T.S., J.E.A., S.A.E. (designed and performed experiments, analyzed the data), J.B. (performed the collagen cross-link analysis), T.M., R.W. (generated rRelm- α), W.B. (performed TEM and 3D confocal studies), A.N. (performed tensile strength assay), A.M. and M.E.R. (provided *Retnla*^{-/-} mice), J.A.K., S.W., T.K., J.E.A., R.R., M.H., S.A.E. (wrote the manuscript).

SUMMARY

Activation of the immune response during injury is a critical early event that determines whether the outcome of tissue restoration is regeneration or replacement of the damaged tissue with a scar. The mechanisms by which immune signals control these fundamentally different regenerative pathways are largely unknown. We have demonstrated that, during skin repair in mice, interleukin-4 receptor α (IL-4R α)-dependent macrophage activation controlled collagen fibril assembly and that this process was important for effective repair while having adverse pro-fibrotic effects. We identified Relm- α as one important player in the pathway from IL-4R α signaling in macrophages to the induction of lysyl hydroxylase 2 (LH2), an enzyme that directs persistent pro-fibrotic collagen cross-links, in fibroblasts. Notably, Relm- β induced LH2 in human fibroblasts, and expression of both factors was increased in lipodermatosclerosis, a condition of excessive human skin fibrosis. Collectively, our findings provide mechanistic insights into the link between type 2 immunity and initiation of pro-fibrotic pathways.

Graphical Abstract



INTRODUCTION

Restoration of tissue integrity and function after injury is a fundamental biological process that is crucial for survival in most organisms. However, there is vast variability between species and tissues in the capacity to regenerate damaged tissue (Tanaka and Reddien, 2011). In particular, mammals are characterized by limited regenerative capacity and tend to replace injured parenchymal cells and extracellular matrix (ECM) with a unique connective tissue defined as scar. Scar tissue is characterized by structural, biochemical, and mechanical alterations that in most circumstances lead to loss of original tissue function. How to avoid the detrimental process of scar formation and promote organ regeneration is still unresolved. Because there is substantial evidence for a negative correlation between immune competence and regenerative capacity (Eming et al., 2009; Medzhitov et al., 2012), the

immune response might offer an important therapeutic target for manipulating the quality of the healing response toward reduced scar formation and improved regeneration. Yet, the mechanisms by which the immune system influences scarring versus regeneration of organ structure and function remains largely unexplained.

In most mammalian tissues, mechanical injury induces a dynamic cellular program proceeding in sequential stages of tissue growth and differentiation (Martin, 1997; Gurtner et al., 2008). The healing response in skin after excisional injury is initiated by a local inflammatory response, followed by the formation of vascularized granulation tissue characterized by myofibroblast differentiation and deposition of provisional ECM that ultimately converts into a persistent fibrous scar tissue. Repair of the dermal tissue is paralleled by regeneration of the overlying epidermis, leading to wound closure.

The type-2-cell-mediated immune response has been identified as a key regulator of progressive fibrosis due to tissue damage in diverse pathological conditions, including chronic asthma, liver fibrosis, and scleroderma (Wynn and Ramalingam, 2012). Type-2-cell-associated immune responses are characterized by the production of interleukin-4 (IL-4) and IL-13, as well as many other T helper 2 (Th2)-cell-associated cytokines, and physiologically have been implicated in important host protective responses, e.g., against helminths (Allen and Maizels, 2011; Chen et al., 2012; Wynn and Ramalingam, 2012; Gause et al., 2013). Helminths, trafficking through host tissues, can cause extensive damage, and from an evolutionary perspective, it has been postulated that the type-2-cell-mediated immune response evolved to facilitate localized restoration of tissue integrity by rapid repair of damaged tissue (Gause et al., 2013). The type-2-cell-mediated immune responses might therefore have a dual role in host protection, including parasite destruction by encapsulation as well as rapid restoration of tissue integrity. The anti-parasitic and wound-healing responses simultaneously produce fibrous matrix and induce scar formation, particularly in those tissues with little regenerative capacity.

Alternative macrophage activation via the IL-4R α has been proposed as a means by which IL-4 and/or IL-13 mediates tissue fibrosis (Gordon, 2003; Wynn, 2004; Wynn and Ramalingam, 2012; Van Dyken and Locksley, 2013), but the detailed mechanisms are unknown. Here, we have shown in a mouse model of excisional skin injury that macrophages alternatively activated via Relm- α production orchestrate pro-fibrotic dihydroxy lysinonorleucine (DHLNL)-collagen crosslinking. This IL-4R α -dependent pathway is critical for the formation of functional granulation tissue but also for its transformation into a persistent scar.

RESULTS

IL-4R α Signaling in Macrophages Is Critical for Skin-Wound Healing

To investigate the role of IL-4 and IL-13 in skin repair, full-thickness-excision skin wounds were inflicted on the backs of control mice (*Il4ra*^{fl/-} or *Il4ra*^{fl/fl}) and mice with complete (*Il4ra*^{-/-}) or myeloid-cell-restricted gene deletion (*Il4ra*^{fl/-}*Lyz2-cre*). Signaling for both cytokines is dependent upon the IL-4R α receptor chain. To characterize the functional impact of IL-4 and IL-13 during the entire time course of the healing response, we

performed wound-tissue analysis during the early (4 days post injury [dpi]), middle (7 dpi), and late phases (14 dpi) of repair.

First, we analyzed expression of IL-4R α in wound tissues during the entire time course of the healing response. Double stainings of wound-tissue sections for IL-4R α and F4/80 (macrophages), CD31 (vascular cells), or α SMA (myofibroblasts) identified macrophages and myofibroblasts as the major cell populations expressing IL-4R α during skin repair (Figures 1A–1C).

To examine whether IL-4R α was expressed in macrophages infiltrating the wound site, we sorted single cell suspensions of CD11b⁺F4/80⁺ cells by flow cytometry from wound tissue of control mice and subjected them to gene-expression analysis by qRT-PCR (Figure S1A). Blood monocytes recruited to the site of skin injury showed a dynamic increase in *Il4ra* expression, peaking with a 3.8 ± 0.6 -fold increase over circulating blood monocytes during the middle stage of repair (Figure 1D). qRT-PCR analysis of macrophages isolated from wound tissue and T and B cells isolated from spleen tissue in *Il4ra^{fl/fl}-Lyz2-cre* mice confirmed efficient myeloid-specific gene deletion during the healing response (Figure 1D; Figure S1B). In addition, disrupted IL-4 and IL-13 responsiveness in macrophages from *Il4ra^{fl/fl}-Lyz2-cre* and *Il4ra^{-/-}* mice was confirmed with functional in vitro assays of macrophage polarization (Figures S1C and S1D).

Morphological analysis by H&E staining of wound-tissue sections during the diverse healing stages revealed major differences in the repair response in control mice versus in IL-4R α -deficient mice. Whereas control mice developed a vascularized and cellular granulation tissue by 7 dpi, in mice with complete or myeloid-cell-restricted *Il4ra* gene deletion, the granulation tissue was highly hemorrhagic (4.3 ± 1.5 -fold and 3.7 ± 1.5 -fold increase of area covered by erythrocytes in *Il4ra^{fl/fl}-Lyz2-cre* and *Il4ra^{-/-}* mice, respectively, in comparison to area covered in controls), indicative of defective granulation-tissue formation and a failure of the repair response (Figures 1E and 1F). Hemorrhages largely resolved during the time course of repair (Figure S2). The disturbed healing response in complete and myeloid-cell-restricted IL-4R α -deficient mice was also evident by a transient delay in wound epithelialization at 4 dpi in these mice when they were compared to controls (Figure 1F). The overall amount of granulation tissue was similar in wounds of control and IL-4R α -deficient mice (Figure 1F).

Analysis of single cell suspensions of wounded tissues by flow cytometry revealed a reduction in the absolute and relative numbers of macrophages (CD11b⁺F4/80⁺ cells) present during the early and middle phases of repair in *Il4ra^{fl/fl}-Lyz2-cre* mice in comparison to those present in controls (Figure 1G). BrdU pulse labeling of wounded mice showed that in wounds of control mice, $6.9\% \pm 1.4\%$ of macrophages proliferated during the early stage of repair and that this process is $27.7\% \pm 21.5\%$ attenuated in mutant mice, suggesting that macrophage proliferation during skin repair is partially controlled by IL-4R α signaling (Figure 1H; Figure S3A). The overall cell number was similar in wounds of control and mutant mice (Figures S3B and S3C). There were no signs of increased bacterial infection in mutant versus control wounds (Figures S3D–S3F).

IL-4R α Signaling in Macrophages Controls Collagen Fibril Formation and Vascular Structures

To investigate the molecular basis for the hemorrhagic phenotype in IL-4R α -deficient mice, we assessed the formation and structure of vascular networks within the granulation tissue by double staining for critical components of vascular integrity (Lindahl et al., 1997; Davis and Senger, 2005), including CD31, perivascular cells (Desmin), and several matrix components of the basement membrane (collagen IV, laminin 1 γ chain, laminin 4 α chain). Whereas the overall quantity of CD31 staining within the granulation tissue in wounds of control and IL-4R α -deficient mice at 7 dpi was comparable (Figure S3G), 3D confocal imaging analysis revealed pronounced differences in the vascular morphology. Whereas, in control mice, the formation of endothelial tubes in network-like structures (vessels) was easily detectable throughout the entire granulation tissue covering up to 79.8% \pm 5.8% of the CD31⁺ area, in IL-4R α -deficient mice, CD31⁺ cells preferentially accumulated in clusters covering up to 54.4% \pm 11.3% in *Il4ra^{fl/-}Lyz2-cre* and 44.8% \pm 4.6% in *Il4ra^{-/-}* mice in the granulation tissue (Figure 2A; Movies S1, S2, and S3). In the gene-deficient mice, tube-like structures were only occasionally detectable toward the wound edge (Figure 2A). In addition, vascular alterations in mutant mice were paralleled by significantly reduced association of CD31⁺ cells with Desmin⁺ perivascular cells in mutant mice when they were compared to controls (Figure 2B). Of note, qRT-PCR analysis of wounded and unwounded skin in *Il4ra^{fl/-}Lyz2-cre* and control mice revealed a reduction of 51.3% \pm 20.5% in *Pdgfb* expression in myeloid-cell-specific *Il4ra* mutants, a factor known to be critical for recruitment of perivascular cells that regulate vascular stability (Figure 2C) (Lindahl et al., 1997). Thus, the formation of functional vascular networks was perturbed in granulation tissue of *Il4ra* mutants.

The morphology of vascular alterations in mutant mice strongly resembled the perturbed vascular phenotype recently described in embryoid bodies generated from β 1-integrin or integrin-linked kinase (ILK)-deficient endothelial cells, which reflects perturbed endothelial-cell-matrix interactions (Malan et al., 2010; Malan et al., 2013). Hence, to examine whether vascular alterations might be associated with structural matrix defects in mutant mice, we performed ultrastructural analysis of wound tissues. Transmission electron microscopy (TEM) analysis revealed profound differences between mouse strains in the morphology of collagen fibrils in wound tissue at 7 and 14 dpi. First, in mutant mice, collagen was less orderly and less densely packed than in control mice (Figure 2D). Second, there was great variability in the shape and size of fibrils in mutant mice; individual fibrils exhibited irregular outlines in cross-section, in contrast to the circular outlines in controls. In some instances, the cross-sectional profiles of collagen fibrils reached very large diameters up to 280–300 nm and showed irregular edges (Figure 2D, asterisk) that were entirely absent in control mice. Third, there was the coexistence of extremely thin collagen fibrils (Figure 2D, arrowheads) intermingled with large ones in mutant mice, whereas in control mice the average size was quite uniform. Quantification of collagen fibril diameters demonstrated that mutant mice exhibited a wider range, with profiles varying from 40–300 nm, whereas control mice contained profiles ranging from 40–200 nm. Collagen fibril morphology was similar in unwounded skin of control and mutant mice. Thus, the absence of IL-4R α signaling in macrophages perturbed collagen fibril formation, which might hamper proper

endothelial-cell-matrix interactions, leading to impaired vascular tube formation and, ultimately, hemorrhages. Finally, numbers of hemosiderin-laden macrophages (indicative of red blood cell [RBC] uptake) were comparable in wounds of control and *Il4ra^{fl/-}Lyz2-cre* mice, making it unlikely that the hemorrhagic phenotype was primarily caused by a RBC removal defect (Figure S3H).

Earlier studies have demonstrated that increased collagen I fibril diameter is related to an enhanced tensile strength in skin and repaired tissues (Bradshaw et al., 2003; Doillon et al., 1988). To examine whether altered collagen fibril architecture in IL-4R α -deficient mice might also impact the biomechanical properties of the scar, we determined tensile strength at 16 dpi. Notably, significantly more force ($26.4\% \pm 14.4\%$) was required to rupture scar tissue derived from mutants versus that from controls (Figure 2E).

IL-4R α Signaling in Macrophages Directs *Plod2* Expression and Collagen Cross-Links in Skin Wounds

On the basis of the disturbed collagen fibrillogenesis, we hypothesized that IL-4R α signaling might control the structural and biochemical assembly of the collagen matrix. We thus examined the expression of collagen-modifying enzymes implicated in this process. Lysyl hydroxylases (LHs, encoded by *Plod* genes) are essential for hydroxylating lysine residues, a process that directs the nature of cross-links of collagen fibers that ultimately define biochemical and structural stability of collagenous tissues (Myllyharju and Kivirikko, 2004). To examine the expression of diverse LH isoforms in skin-wound healing, we subjected wounded and unwounded skin of *Il4ra^{fl/-}Lyz2-cre* and control mice to qRT-PCR analysis. Whereas wounding of control and mutant mice did not lead to significant induction of LH1 (*Plod1*) and LH3 (*Plod3*) expression, LH2 (long) (*Plod2*) expression in control mice peaked with a 215 ± 115 -fold induction during the middle stage of repair (Figure 3A). Notably, *Plod2* expression in wounds of *Il4ra^{fl/-}Lyz2-cre* mice was $76.1\% \pm 11.5\%$ and $47.7\% \pm 11.7\%$ reduced at 7 and 14 dpi, respectively, in comparison to expression in control mice (Figure 3A). Attenuated *Plod2* expression in wounds of *Il4ra^{fl/-}Lyz2-cre* mice was confirmed by weak immunohisto-chemical staining for LH2 in granulation tissue of mutant mice in comparison to a strong staining signal in control mice (Figures 3B and 3C).

LH2 is the only enzyme known that hydroxylates lysine residues specifically in the telopeptides of collagen polypeptides, a process that is essential to direct dihydroxy lysinonorleucine (DHLNL) cross-links of collagen fibrils (van der Slot et al., 2003; Pornprasertsuk et al., 2004; Pornprasertsuk et al., 2005). DHLNL collagen cross-links are a typical feature of mechanically stiff tissues such as bone and cartilage and are virtually absent in human soft connective tissues such as normal skin, which is characterized by lysine-aldehyde-derived collagen cross-links (hydroxylysine, HLNL) (Myllyharju and Kivirikko, 2004). In human skin, identification of DHLNL collagen cross-links has been limited to pathological conditions such as lipodermato-sclerosis (skin fibrosis associated with chronic venous insufficiency) or scleroderma (Brinckmann et al., 1999; van der Slot et al., 2004). Here, we have shown that in unwounded and wounded skin of control and mutant mice, the concentration of HLNL per collagen was similar and not altered during the repair response (Figure 3D). In contrast, DHLNL collagen cross-links were detected at low

amounts in unwounded skin of control mice and increased 1.9 ± 0.3 -fold and 3.1 ± 0.5 -fold in granulation tissue 5 and 10 dpi (Figure 3D), respectively. In mutant mice, DHLNL cross-links were also detectable in unwounded skin, in comparable amounts to those detected in controls (Figure 3D). However, DHLNL collagen cross-links were significantly attenuated in wound tissue of mutant mice when compared to that in controls (Figure 3D). Collectively, we found that IL-4 and IL-13 responsiveness in macrophages controlled *Plod2* expression in skin wounds and determined the nature of collagen cross-links.

Attenuated Alternative Macrophage Activation in Late-Stage Skin-Wound Healing in *Il4ra^{fl/-}Lyz2-cre* Mice

To investigate whether impaired granulation tissue formation and defective collagen fibrillogenesis in *Il4ra^{fl/-}Lyz2-cre* mice is associated with altered macrophage activation during healing progression, CD11b⁺F4/80⁺ cells from wound tissue were sorted by flow cytometry and subjected to qRT-PCR analysis. Gene expression of wound macrophages was correlated with gene expression in circulating blood monocytes (SSC^{low}CD11b⁺) from unwounded mice and sorted by flow cytometry. Consistent with earlier reports from our group and others (Lucas et al., 2010; Willenborg et al., 2012), early and late-stage wound macrophages are characterized by a distinct gene-expression profile reflecting classical and alternative activation during the early and late phase of repair, respectively (Figure 4A). In control mice, expression of genes characterizing alternative activation, including *Cd163*, *Retna*, *Cd206*, and *Il10*, was low during the early stage of repair (4 dpi) and dynamically upregulated toward 14 dpi (Figure 4A). Furthermore, early stage wound macrophages were characterized by a 27.7 ± 18.1 -fold induction of *Nos2* expression (characterizing classical activation) that declined over the time course of healing (Figure 4A). In contrast, in *Il4ra^{fl/-}Lyz2-cre* mice, alternative polarization of late-stage wound macrophages was significantly attenuated in comparison to polarization in control mice, whereas in early stage wound macrophages, *Nos2* expression was significantly upregulated and prolonged in comparison to expression in controls (4 dpi, 5.1 ± 2.2 -fold increase and 7 dpi, 8.1 ± 4.7 -fold increase, respectively, over controls). Of note, other genes characterizing early stage classical activation, such as *Il1b*, *Tnf*, and *Il6*, were not differentially expressed in control or mutant mice (Figure S4).

Relm- α Derived from Middle- and Late-Stage-Activated Wound Macrophages Directs *Plod2* Expression in Fibroblasts

To explore the hypothesis that defective collagen fibril cross-linking in *Il4ra^{fl/-}Lyz2-cre* mice is mediated by an altered cross-talk between macrophages and fibroblasts, we used an in vitro co-culture system, in which the cell types have no direct contact. *Plod2* expression was assessed by qRT-PCR in skin fibroblasts after exposure to classically (IFN- γ and LPS) or alternatively (IL-4 and IL-13) activated macrophages. *Plod2* expression in fibroblasts (isolated from *Il4ra^{-/-}* mice) was 1.4 ± 0.1 -fold upregulated upon exposure to IL-4- and IL-13-activated macrophages in comparison to expression in fibroblasts not exposed to macrophages or exposed to macrophages cultured in vehicle or activated with IFN- γ and LPS (Figure 4B). Consistently, *Plod2* expression in fibroblasts was not detected when co-cultured with IL-4- and IL-13-treated macrophages isolated from IL-4R α -deficient mice (Figure 4B).

We next examined candidate macrophage-derived signals that might induce *Plod2* expression in fibroblasts. Although in vitro studies have reported that TGF- β 1 can induce *Plod2* expression in fibroblasts (van der Slot et al., 2005a), *Tgfb1* expression was not upregulated in IL-4- and IL-13-activated macrophages in our model (data not shown). In contrast, *Retnla*, the gene encoding a small cysteine-rich secreted molecule that is a hallmark of alternatively activated macrophages (Gordon, 2003) and has been associated with experimental fibrosis (Liu et al., 2004) and pro-fibrotic conditions in human diseases (Angelini et al., 2009; Kushiyama et al., 2013; Fang et al., 2015), was continuously upregulated in wound macrophages during the time course of repair (Figure 4A). Therefore, we tested whether Relm- α released by IL-4- and IL-13-activated macrophages controlled *Plod2* expression in fibroblasts. We first showed that *Retnla* could be effectively silenced by siRNA in macrophages, stimulated with IL-4 and IL-13, and co-cultured with fibroblasts (Figure 4C). Notably, IL-4- and IL-13-stimulated macrophages transfected with Relm- α siRNA failed to induce *Plod2* expression in fibroblasts, whereas control macrophages transfected with scrambled RNA induced expression of *Plod2* in fibroblasts (Figure 4C). To corroborate the finding that Relm- α induced *Plod2* expression in fibroblasts, we exposed fibroblasts to recombinant murine Relm- α (rRelm- α). Stimulation of fibroblasts with rRelm- α induced *Plod2* expression up to 1.6 ± 0.2 -fold in comparison to expression in the control (Figure 4D).

Local Application of rRelm- α Rescues Wound-Healing Pathology and Attenuated *Plod2* Expression in *Il4ra^{fl/-}Lyz2-cre* Mice

We next investigated whether myeloid-cell-restricted IL-4R α signaling is critical for Relm- α -mediated orchestration of granulation tissue formation and collagen fibril assembly. For this purpose, wound tissue of *Il4ra^{fl/-}Lyz2-cre* and control mice was subjected to qRT-PCR analysis to quantify *Retnla* expression. Whereas in control mice *Retnla* expression was upregulated during the time course of healing, the expression was significantly reduced in wounds of *Il4ra^{fl/-}Lyz2-cre* mice at 7 and 14 dpi, respectively (Figure 5A). Consistent with reduced *Retnla* expression in purified wound macrophages in *Il4ra^{fl/-}Lyz2-cre* mice (Figure 4A), immunohistochemical staining of wound tissues showed a reduced number of Relm- α ⁺F4/80⁺ double-positive cells within the granulation tissue of *Il4ra^{fl/-}Lyz2-cre* mice in comparison to that in control mice (Figures 5B and 5C).

To address whether local application of rRelm- α could rescue impaired granulation tissue formation in *Il4ra^{fl/-}Lyz2-cre* mice, we injected the edges of wounds in *Il4ra^{fl/-}Lyz2-cre* mice twice (3 and 5 dpi) with rRelm- α (1 μ g/wound) or vehicle, and the repair response was assessed. H&E staining of wound-tissue sections at 7 dpi revealed that rRelm- α treatment normalized hemorrhages within the granulation tissue of *Il4ra^{fl/-}Lyz2-cre* mice (Figures 1E and 1F, Figures 5D and 5E). The number of wound macrophages (CD68⁺ cells) was comparable in granulation tissue in vehicle- or rRelm- α -injected *Il4ra^{fl/-}Lyz2-cre* mice, suggesting that the resolution of the hemorrhages is not due to increased macrophage numbers (Figure 5F).

We then tested whether the normalized wound phenotype in rRelm- α -treated wounds in *Il4ra^{fl/-}Lyz2-cre* mice was associated with increased local *Plod2* expression. qRT-PCR

analysis of complete wound tissue revealed that, indeed, *Plod2* expression was 9.7 ± 3.7 -fold upregulated in comparison to expression in vehicle-treated wounds in *Il4ra^{fl/fl}-Lyz2-cre* mice. In fact, *Plod2* expression was restored to an amount similar to that in *Il4ra^{fl/fl}* mice at 7 dpi (Figure 3A, Figure 5G).

The Disturbed Healing Phenotype Is Similar in *Il4ra^{fl/fl}-Lyz2-cre* and *Retnla*-Deficient Mice

To substantiate a direct role of Relm- α in skin repair, we characterized the wound-healing response in *Retnla^{-/-}* mice. Notably, we detected intriguing parallels regarding morphological, structural, and biochemical alterations of the wound-healing response in *Retnla^{-/-}* and *Il4ra^{fl/fl}-Lyz2-cre* mice (Figure 6). As such, the repair response in *Retnla^{-/-}* mice was characterized by a highly hemorrhagic granulation tissue (Figures 6A and 6B), transient delay in wound epithelialization (Figure 6C), altered assembly and size of collagen fibrils (Figure 6D), reduced DHLNL collagen cross-links (Figure 6E), $39.0\% \pm 30.7\%$ reduced expression of *Plod2* (Figure 6F) and $22.4\% \pm 18.8\%$ increased tensile strength (Figure 6G). Expression of inflammatory mediators including *Il6*, *Tnf*, and *Il1b*, numbers of inflammatory cells (F4/80⁺ or Gr1⁺), and hemosiderin laden macrophages were comparable in wound tissue in control and *Retnla^{-/-}* mice (Figure S5). Collectively, these findings demonstrate a direct role of Relm- α in rapid and effective restoration of tissue integrity and support our hypothesis that impaired wound healing in *Il4ra^{fl/fl}-Lyz2-cre* mice is at least in part mediated by a reduction of Relm- α .

To investigate whether initiation of pro-fibrotic pathways by Relm- α might also apply to humans, we examined the effect of rRelm- β (1 μ g/mL, 24 hr), the human homolog of murine Relm- α (Holcomb et al., 2000), on gene expression in human dermal fibroblasts. rRelm- β induced a $30.0\% \pm 18.5\%$ increased expression of *PLOD2* and $22.6\% \pm 15.1\%$ increased expression of *ACTA2* (α -smooth muscle actin) (Figure 6H). In addition, we quantified expression of *RETNLB* and of *PLOD2* in tissue samples of lipodermatosclerosis (excessive skin fibrosis associated with chronic venous insufficiency) and healthy human skin by qRT-PCR analysis (Figure 6I). Indeed, expression of both genes was 2.8 ± 2.2 -fold and 4.2 ± 1.9 -fold upregulated in fibrotic skin in comparison to expression in normal skin, suggesting a potential relevance in the pathology of this human fibrotic skin condition.

DISCUSSION

Here, we have shown that, after mechanical skin injury, IL-4R α signaling coordinated the timely switch from an inflammatory toward a resolution phenotype in macrophages. We found that defective wound healing in *Il4ra^{fl/fl}-Lyz2-cre* mice was primarily due to a failure of macrophages to initiate an essential repair program, rather than unrestrained pro-inflammatory responses as reported in a model of excessive helminth-induced lung damage in IL-4R α -deficient mice (Chen et al., 2012). We further identified Relm- α as one critical factor released by IL-4- and IL-13-stimulated macrophages for a timely and effective wound-healing response.

An unexpected and important finding of our work was that IL-4 and IL-13 signaling in wound macrophages controlled the architecture of collagen fibrils and the biochemistry of collagen cross-links. Our findings suggest that alterations of these matrix properties

functionally impact both the early and the late stages of repair. Disruption during the early repair phase was evidenced by perturbed formation of vessels causing hemorrhages during granulation tissue development. Alterations in late-stage repair were revealed by increased tensile strength of scar tissue. Type-2-cell-mediated immune signals have been widely associated with altered ECM morphology and tissue fibrosis in various experimental and human disease conditions (Wynn, 2004; Wynn and Ramalingam, 2012; Brinckmann et al., 2005). However, studies have focused primarily on the quantitative assessment of the amount of collagen deposition, rather than potential effects of type-2-cell-mediated immune signals on post-translational collagen modifications that impact matrix architecture and function. Collagen fibril biosynthesis is a complex and multistep process of fundamental importance during embryonic development and tissue remodeling, providing structural and biochemical stability and function to tissues and organs (Myllyharju and Kivirikko, 2004). Our study in skin gives mechanistic insights into the regulation of this process at several levels. We have provided direct evidence that mediators released upon IL-4 and IL-13-mediated macrophage activation, particularly Relm- α , induce expression of the collagen-modifying enzyme LH2 in fibroblasts. DHLNL collagen cross-links mediated by LH2 are thought to be critical for the determination of the structural, biochemical, and mechanical properties of fibrillar collagens, and their biological significance has been demonstrated in disease processes with tissue fragility or fibrosis with altered *PLOD2* expression (Brinckmann et al., 2001; van der Slot et al., 2003; van der Slot- Verhoeven et al., 2005b). We think that the hemorrhagic phenotype of the early granulation tissue in *Il4ra^{fl/fl}-Lyz2-cre* mice is caused by attenuated DHLNL cross-linking. Reduced DHLNL cross-links result in defective structural and organizational stability of the ECM, which is crucial for proper endothelial-cell-matrix interactions during the formation of a vascular network (Davis and Senger, 2005). The reduction of endothelial-tube-like structures and increased assembly of endothelial cells in clusters in granulation tissue of mutant mice resembled the perturbed formation of vascular networks that result from disturbed endothelial-cell-matrix interactions in β 1-integrin or ILK-deficient endothelial cells (Malan et al., 2010; Malan et al., 2013). Our findings indicate that in IL-4R α -deficient mice, disturbed collagen fibril architecture also leads to perturbed endothelial-cell fibril contacts with the consequence of disturbed tube formation, vascular integrity, and ultimately increased leakage. This assumption is supported in mice with a body-wide heterozygous deficiency for LH2 and that are characterized by severe vascular defects, decreased DHLNL collagen cross-links, and disturbed collagen fibrillogenesis (Hyry, 2012).

Furthermore, the diameter of collagen fibrils was severely altered and tensile strength of scar tissue was increased in *Il4ra* mutant mice. These findings are consistent with earlier studies demonstrating that increased collagen I fiber diameter is related to an enhanced tensile strength in skin and repaired tissue (Bradshaw et al., 2003; Doillon et al., 1988). Therefore, the higher tensile strength we observed in mutant mice is most likely due to the increased proportion of collagen fibrils with an increased diameter in the scar tissue. Thus, in the absence of IL-4R α signaling, alterations in the fibril diameter might contribute more to tensile strength than the amount of cross-links. Hence, at this stage we conclude that IL-4R α controls restoration of tissue architecture and its mechanical properties.

We identified Relm- α as one critical factor by which alternatively activated macrophages in mouse wounds mediate *Plod2* expression in fibroblasts. We therefore propose that Relm- α initiates a pathway that is involved in collagen fibrillogenesis and cross-linking, thus determining structural and biochemical stability of the newly forming tissue. In support of this hypothesis, hemorrhages and attenuated *Plod2* expression in middle-stage wounds of myeloid-cell-restricted IL-4R α -deficient mice were rescued by local application of rRelm- α . Importantly, *Retnla*^{-/-} mice displayed wound healing alterations very similar to those in *Il4ra*^{fl/-}*Lyz2-cre* mice. These findings strongly suggest that attenuated Relm- α synthesis in myeloid-cell-restricted IL-4R α -deficient mice is responsible for attenuated *Plod2* expression in fibroblasts and eventually its sequelae of altered matrix architecture and function. In support of a pro-fibrotic role of Relm- α , increased *Retnla* expression has been associated with several fibrotic conditions and fibroplasia in experimental mouse models and human disease (Liu et al., 2004; Kushiyama et al., 2013). We show here that in human skin fibroblasts, rRelm- β (the human homolog of murine Relm- α) induces *PLOD2* expression, and even more importantly, in lipodermatosclerosis, a pronounced skin fibrosis in patients with chronic venous insufficiency that is associated with increased DHLNL cross-links (Brinckmann et al., 2001), *RETLNB* and *PLOD2* are significantly upregulated in comparison to their presence in healthy skin. Thus, our findings provide insights into mechanisms by which Relm- α controls matrix architecture and promotes tissue fibrosis, possibly identifying an important therapeutic target to treat conditions of tissue fibrosis.

We show that, in injured mouse skin, myeloid-cell-restricted IL-4R α signaling controls both pathways that facilitate rapid restoration of tissue integrity but also simultaneously leads to scar formation. This differs from two recent studies reporting that type-2-cell-mediated signals facilitate skeletal muscle and liver regeneration in mice, both processes that naturally occur without scar formation (Heredia et al., 2013; Goh et al., 2013). In those tissues, parenchymal cells, not macrophages, appeared to be the direct and critical targets of IL-4 during organ regeneration. Importantly, in contrast to skeletal muscle and the liver, the dermal component of skin has limited regenerative capacity in mammals, thus healing by scar formation. Altogether, these findings lead to the intriguing hypothesis that type-2-cell-mediated immune signals promote and facilitate restoration of tissue integrity after injury, but in organs with limited intrinsic regenerative capacity, such as mammalian dermis, the process also drives cellular pathways that are critical to scar formation.

EXPERIMENTAL PROCEDURES

Animals

Myeloid-cell-specific IL-4R α -deficient mice (*Il4ra*^{fl/-}*Lyz2-cre*) and *Retnla*^{-/-} mice (BALB/c background, 10–12 weeks) were generated and genotyped as previously described (Figure S6 and Supplemental References). All procedures were approved by the North Rhine-Westphalian State Agency for Nature, Environment, and Consumer Protection and the University of Cologne.

Cell Culture

Primary dermal fibroblasts were isolated from the back skin of mice and from the skin of two different human donors. Macrophages were isolated from the peritoneal cavity by plastic adhesion or from the bone marrow (BMDM). Stimulation of cells and the co-culture system are described in the Supplemental Experimental Procedures.

Relm- α Silencing by siRNA

BMDM were transfected via the Nucleofector Kit (Lonza) with either Relm- α targeted siRNA or scrambled siRNA (Thermo Scientific Dharmacon). Details are described in the Supplemental Experimental Procedures.

Wounding

Wounding, preparation of wound tissue for histology, and morphometric analysis was performed as described previously (Willenborg et al., 2012). For local treatment of wounds with rRelm- α , wound edges were injected either with rRelm- α (1 μ g in 50 μ L PBS) or vehicle (50 μ L PBS) at 3, 4, and 5 dpi.

Lipodermatosclerosis

Human tissue samples were obtained from patients presenting with lipodermatosclerosis. After collection, tissues were snap-frozen in liquid nitrogen or stored in RNAlater (Life Technologies). RNA was isolated with the Fibrous Tissue Mini Kit (QIAGEN). The study was approved by the Ethics Committee of the Medical Faculty of the University of Cologne and informed consent of patients was received.

Immunohistochemistry

Immunohistochemical stainings (10 μ m and 40 μ m cryosections) were performed as described previously (Willenborg et al., 2012). Confocal microscopy for 3D imaging of the endothelial tubes and clusters was performed as described previously (Malan et al., 2013) by performing z-stacks and subsequent use of 3D projection function of the LSM 510 Meta (Zeiss). Antibodies and analysis of stained sections, Gram staining, and iron staining are described in the Supplemental Experimental Procedures.

Electron Microscopy

Tissue was fixed and processed according to a standard protocol. After tissue was embedded in Epon-Araldite, ultrathin sections (50–100 nm) were analyzed via a Zeiss 902A Transmission Electron Microscope (Zeiss) and TEM Imaging Platform iTEM Software (Soft Imaging Systems).

Flow Cytometry

Flow cytometry and cell sorting were performed as described previously (Willenborg et al., 2012). FACS analysis and cell sorting was performed with the BD FACS Canto II flow cytometer, the BD FACS Aria III cell sorter, and the BD FACS Diva Software. Antibodies used are listed in the Supplemental Experimental Procedures.

Real-time PCR Analysis

RNA from complete wound tissue was isolated with the Fibrous Tissue Mini Kit, and RNA from single cell suspensions was isolated with the RNeasy Mini or Micro Kits (QIAGEN). Reverse transcription and qRT-PCR analysis are described in the Supplemental Experimental Procedures.

Collagen Cross-Link Analysis

Collagen cross-link analysis was performed as previously described (Brinckmann et al., 2005). Tissue specimens (about 20 mg wet weight) were reduced, denatured, and digested. Analysis was performed with an amino acid analyzer (Biochrom 20). Details are described in the Supplemental Experimental Procedures.

Recombinant Relm- α

Recombinant murine rRelm- α was expressed in HEK293-EBNA cells and purified from cell culture supernatant. The identity of the purified recombinant protein was confirmed by western blot with anti Relm- α (Peprotech). Details are described in the Supplemental Experimental Procedures.

Tensile Strength Test

Incisional wounds (length: 2 cm) were placed on the backs of mutant mice. At 16 dpi, two identical rectangle-shaped (1 cm \times 2.5 cm) pieces of the back skin with scar tissue located in the center were excised and stored in isotonic NaCl solution at -20°C . Thawed specimens underwent a tensile strength test via a material testing machine (Z2.5/TN1S, Zwick). After preloading (0.05 N, 0.1 mm/s), the scar tissue was stretched until failure with a cross-head speed of 15 mm/min.

Statistical Analysis

Statistical analysis was performed with the Student's paired or unpaired two-tailed t test or ANOVA one-way test analysis with Dunnett's Multiple Comparison Test. In case of not assumed equal variances, a Welch correction was performed. Data are presented as the mean and, where indicated, with \pm SD, and significance levels are indicated in each figure.

Supplementary Material

Refer to Web version on PubMed Central for supplementary material.

Acknowledgments

The authors thank Michael Piekarek, Sebastian Wüst, Christoph Göttlinger, and Gunter Rappl (Central Cell Sorting Facility, Center for Molecular Medicine Cologne, University of Cologne) for excellent technical assistance. The authors are grateful to Dr. Brombacher for providing *Il4ra^{fl/fl}* mice and Dr. Irmgard Förster for providing *Lyz2-cre* mice, Regeneron Pharmaceuticals for providing the *Retnla^{-/-}* mice, Dr. Peter Bruckner and Dr. Uwe Hansen for advice in ECM analysis, and Dr. David Artis and Dr. Meera Nair for providing the plasmid of murine Relm- α . The main funding source for this manuscript was the Deutsche Forschungsgemeinschaft (SFB829 to S.A.E., T.K., R.W., and M.H.), J.E.A. and T.S. were supported by the Medical Research Council (MR/J001929/1) and M.E.R. by NIH R37 AI045898.

References

- Allen JE, Maizels RM. Diversity and dialogue in immunity to helminths. *Nat Rev Immunol.* 2011; 11:375–388. [PubMed: 21610741]
- Angelini DJ, Su Q, Yamaji-Kegan K, Fan C, Teng X, Hassoun PM, Yang SC, Champion HC, Tuder RM, Johns RA. Resistin-like molecule-beta in scleroderma-associated pulmonary hypertension. *Am J Respir Cell Mol Biol.* 2009; 41:553–561. [PubMed: 19251945]
- Bradshaw AD, Puolakkainen P, Dasgupta J, Davidson JM, Wight TN, Helene Sage E. SPARC-null mice display abnormalities in the dermis characterized by decreased collagen fibril diameter and reduced tensile strength. *J Invest Dermatol.* 2003; 120:949–955. [PubMed: 12787119]
- Brinckmann J, Notbohm H, Tronnier M, Açil Y, Fietzek PP, Schmeller W, Müller PK, Bätge B. Overhydroxylation of lysyl residues is the initial step for altered collagen cross-links and fibril architecture in fibrotic skin. *J Invest Dermatol.* 1999; 113:617–621. [PubMed: 10504450]
- Brinckmann J, Neess CM, Gaber Y, Sobhi H, Notbohm H, Hunzelmann N, Fietzek PP, Müller PK, Risteli J, Gebker R, Scharffetter-Kochanek K. Different pattern of collagen cross-links in two sclerotic skin diseases: lipodermatosclerosis and circumscribed scleroderma. *J Invest Dermatol.* 2001; 117:269–273. [PubMed: 11511304]
- Brinckmann J, Kim S, Wu J, Reinhardt DP, Batmunkh C, Metzen E, Notbohm H, Bank RA, Krieg T, Hunzelmann N. Interleukin 4 and prolonged hypoxia induce a higher gene expression of lysyl hydroxylase 2 and an altered cross-link pattern: important pathogenetic steps in early and late stage of systemic scleroderma? *Matrix Biol.* 2005; 24:459–468. [PubMed: 16139999]
- Chen F, Liu Z, Wu W, Rozo C, Bowdridge S, Millman A, Van Rooijen N, Urban JF Jr, Wynn TA, Gause WC. An essential role for TH2-type responses in limiting acute tissue damage during experimental helminth infection. *Nat Med.* 2012; 18:260–266. [PubMed: 22245779]
- Davis GE, Senger DR. Endothelial extracellular matrix: biosynthesis, remodeling, and functions during vascular morphogenesis and neovessel stabilization. *Circ Res.* 2005; 97:1093–1107. [PubMed: 16306453]
- Doillon CJ, Dunn MG, Silver FH. Relationship between mechanical properties and collagen structure of closed and open wounds. *J Biomech Eng.* 1988; 110:352–356. [PubMed: 3205021]
- Eming SA, Hammerschmidt M, Krieg T, Roers A. Interrelation of immunity and tissue repair or regeneration. *Semin Cell Dev Biol.* 2009; 20:517–527. [PubMed: 19393325]
- Fang CL, Yin LJ, Sharma S, Kierstein S, Wu HF, Eid G, Haczku A, Corrigan CJ, Ying S. Resistin-like molecule- β (RELM- β) targets airways fibroblasts to effect remodelling in asthma: from mouse to man. *Clin Exp Allergy.* 2015; 45:940–952. [PubMed: 25545115]
- Gause WC, Wynn TA, Allen JE. Type 2 immunity and wound healing: evolutionary refinement of adaptive immunity by helminths. *Nat Rev Immunol.* 2013; 13:607–614. [PubMed: 23827958]
- Goh YP, Henderson NC, Heredia JE, Red Eagle A, Odegaard JI, Lehwald N, Nguyen KD, Sheppard D, Mukundan L, Locksley RM, Chawla A. Eosinophils secrete IL-4 to facilitate liver regeneration. *Proc Natl Acad Sci USA.* 2013; 110:9914–9919. [PubMed: 23716700]
- Gordon S. Alternative activation of macrophages. *Nat Rev Immunol.* 2003; 3:23–35. [PubMed: 12511873]
- Gurtner GC, Werner S, Barrandon Y, Longaker MT. Wound repair and regeneration. *Nature.* 2008; 453:314–321. [PubMed: 18480812]
- Heredia JE, Mukundan L, Chen FM, Mueller AA, Deo RC, Locksley RM, Rando TA, Chawla A. Type 2 innate signals stimulate fibro/adipogenic progenitors to facilitate muscle regeneration. *Cell.* 2013; 153:376–388. [PubMed: 23582327]
- Holcomb IN, Kabakoff RC, Chan B, Baker TW, Gurney A, Henzel W, Nelson C, Lowman HB, Wright BD, Skelton NJ, et al. FIZZ1, a novel cysteine-rich secreted protein associated with pulmonary inflammation, defines a new gene family. *EMBO J.* 2000; 19:4046–4055. [PubMed: 10921885]
- Hyry, M. PhD thesis. Oulu: University of Oulu; 2012. Lysyl hydroxylases 1 and 2: characterization of their in vivo roles in mouse and the molecular level consequences of the lysyl hydroxylase 2 mutations found in Bruck syndrome.

- Kushiyama A, Sakoda H, Oue N, Okubo M, Nakatsu Y, Ono H, Fukushima T, Kamata H, Nishimura F, Kikuchi T, et al. Resistin-like molecule β is abundantly expressed in foam cells and is involved in atherosclerosis development. *Arterioscler Thromb Vasc Biol.* 2013; 33:1986–1993. [PubMed: 23702657]
- Lindahl P, Johansson BR, Levéen P, Betsholtz C. Pericyte loss and microaneurysm formation in PDGF-B-deficient mice. *Science.* 1997; 277:242–245. [PubMed: 9211853]
- Liu T, Jin H, Ullenbruch M, Hu B, Hashimoto N, Moore B, McKenzie A, Lukacs NW, Phan SH. Regulation of found in inflammatory zone 1 expression in bleomycin-induced lung fibrosis: role of IL-4/IL-13 and mediation via STAT-6. *J Immunol.* 2004; 173:3425–3431. [PubMed: 15322207]
- Lucas T, Waisman A, Ranjan R, Roes J, Krieg T, Müller W, Roers A, Eming SA. Differential roles of macrophages in diverse phases of skin repair. *J Immunol.* 2010; 184:3964–3977. [PubMed: 20176743]
- Malan D, Wenzel D, Schmidt A, Geisen C, Raible A, Bölc B, Fleischmann BK, Bloch W. Endothelial beta1 integrins regulate sprouting and network formation during vascular development. *Development.* 2010; 137:993–1002. [PubMed: 20179098]
- Malan D, Elischer A, Hesse M, Wickström SA, Fleischmann BK, Bloch W. Deletion of integrin linked kinase in endothelial cells results in defective RTK signaling caused by caveolin 1 mislocalization. *Development.* 2013; 140:987–995. [PubMed: 23404105]
- Martin P. Wound healing—aiming for perfect skin regeneration. *Science.* 1997; 276:75–81. [PubMed: 9082989]
- Medzhitov R, Schneider DS, Soares MP. Disease tolerance as a defense strategy. *Science.* 2012; 335:936–941. [PubMed: 22363001]
- Myllyharju J, Kivirikko KI. Collagens, modifying enzymes and their mutations in humans, flies and worms. *Trends Genet.* 2004; 20:33–43. [PubMed: 14698617]
- Pornprasertsuk S, Duarte WR, Mochida Y, Yamauchi M. Lysyl hydroxylase-2b directs collagen cross-linking pathways in MC3T3-E1 cells. *J Bone Miner Res.* 2004; 19:1349–1355. [PubMed: 15231023]
- Pornprasertsuk S, Duarte WR, Mochida Y, Yamauchi M. Overexpression of lysyl hydroxylase-2b leads to defective collagen fibrillogen-esis and matrix mineralization. *J Bone Miner Res.* 2005; 20:81–87. [PubMed: 15619673]
- Tanaka EM, Reddien PW. The cellular basis for animal regeneration. *Dev Cell.* 2011; 21:172–185. [PubMed: 21763617]
- van der Slot AJ, Zuurmond AM, Bardoel AF, Wijmenga C, Pruijs HE, Sillence DO, Brinckmann J, Abraham DJ, Black CM, Verzijl N, et al. Identification of PLOD2 as telopeptide lysyl hydroxylase, an important enzyme in fibrosis. *J Biol Chem.* 2003; 278:40967–40972. [PubMed: 12881513]
- van der Slot AJ, Zuurmond AM, van den Bogaerd AJ, Ulrich MM, Middelkoop E, Boers W, Karel Runday H, DeGroot J, Huizinga TW, Bank RA. Increased formation of pyridinoline cross-links due to higher telopeptide lysyl hydroxylase levels is a general fibrotic phenomenon. *Matrix Biol.* 2004; 23:251–257. [PubMed: 15296939]
- van der Slot AJ, van Dura EA, de Wit EC, De Groot J, Huizinga TW, Bank RA, Zuurmond AM. Elevated formation of pyridinoline cross-links by profibrotic cytokines is associated with enhanced lysyl hydroxylase 2b levels. *Biochim Biophys Acta.* 2005a; 1741:95–102. [PubMed: 15955452]
- van der Slot-Verhoeven AJ, van Dura EA, Attema J, Blauw B, Degroot J, Huizinga TW, Zuurmond AM, Bank RA. The type of collagen cross-link determines the reversibility of experimental skin fibrosis. *Biochim Biophys Acta.* 2005b; 1740:60–67. [PubMed: 15878742]
- Van Dyken SJ, Locksley RM. Interleukin-4- and interleukin-13-mediated alternatively activated macrophages: roles in homeostasis and disease. *Annu Rev Immunol.* 2013; 31:317–343. [PubMed: 23298208]
- Willenborg S, Lucas T, van Loo G, Knipper JA, Krieg T, Haase I, Brachvogel B, Hammerschmidt M, Nagy A, Ferrara N, et al. CCR2 recruits an inflammatory macrophage subpopulation critical for angiogenesis in tissue repair. *Blood.* 2012; 120:613–625. [PubMed: 22577176]

Wynn TA. Fibrotic disease and the T(H)1/T(H)2 paradigm. *Nat Rev Immunol.* 2004; 4:583–594. [PubMed: 15286725]

Wynn TA, Ramalingam TR. Mechanisms of fibrosis: therapeutic translation for fibrotic disease. *Nat Med.* 2012; 18:1028–1040. [PubMed: 22772564]

Author Manuscript

Author Manuscript

Author Manuscript

Author Manuscript

Highlights

- Type 2 immune signals are critical for macrophage polarization in skin-wound healing
- Myeloid-cell-restricted IL-4R α signaling controls collagen fibril assembly
- Macrophage-derived Relm- α controls LH2-mediated profibrotic collagen cross-linking
- Expression of human Relm- β and LH2 is increased in lipodermatosclerosis

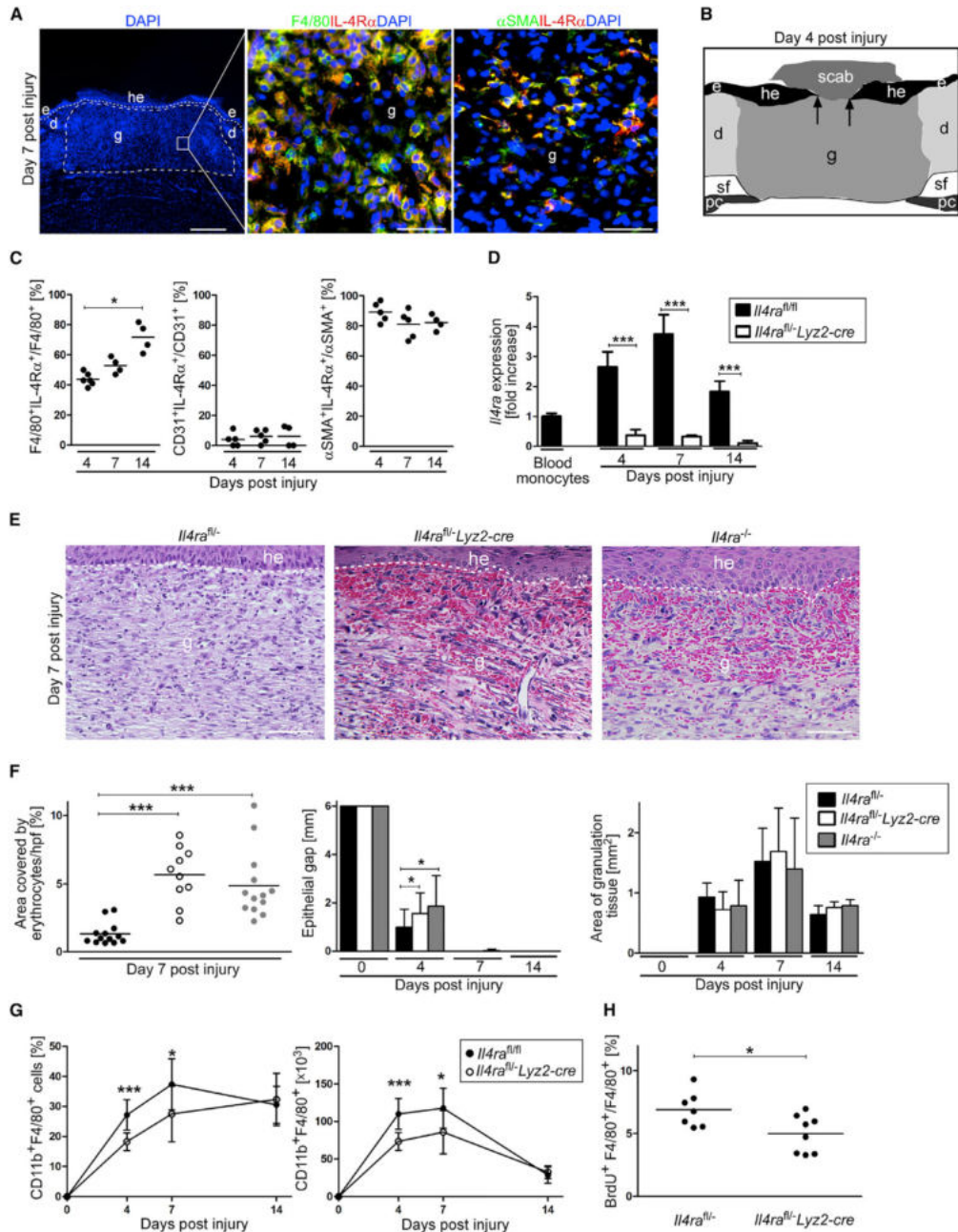


Figure 1. IL-4Rα Signaling in Macrophages Is Critical for Skin-Wound Healing

(A) IHC double staining on wound sections at 7 dpi; (left) scale bar represents 500 μm, (right) scale bar represents 40 μm.
 (B) Scheme illustrating histology of excisional skin wound.
 (C) Quantification of double-positive cells in wound tissue in control mice (n = 4–6 wounds of 2–4 mice per time point).
 (D) *Il4ra* gene expression of flow-cytometry-sorted CD11b⁺F4/80⁺ wound macrophages at indicated dpi (n = 3–7 wounds of 3–6 mice per genotype and time point).
 (E) Representative H&E staining of granulation tissue at 7 dpi; scale bar represents 50 μm.

(F) Quantification of hemorrhages in the granulation tissue and morphometric analysis of wound closure kinetics and quantification of granulation tissue (4 and 7 dpi) and scar (14 dpi) formation at indicated dpi (n = 14–23 wounds of 7–12 mice per genotype and time point).

(G) Flow cytometry analysis of wound cell suspensions; frequency and absolute number of CD11b⁺F4/80⁺ cells at indicated dpi (n = 4–10 wounds of 4–8 mice).

(H) Frequency of BrdU⁺F4/80⁺ wound macrophages at 4 dpi, based on flow cytometry analysis. d, dermis; e, epidermis; g, granulation tissue; he, hyper-proliferative epithelium; pc, panniculus carnosus; sf, subcutaneous fat tissue. The dashed line indicates the junction between the epidermis and dermis, arrows indicate the tip of the epithelial tongue, and each dot represents one wound. Data are expressed as the mean and, where indicated, with \pm SD. *p < 0.05; ***p < 0.001. This figure is supported by Figures S1–S3 and S6.

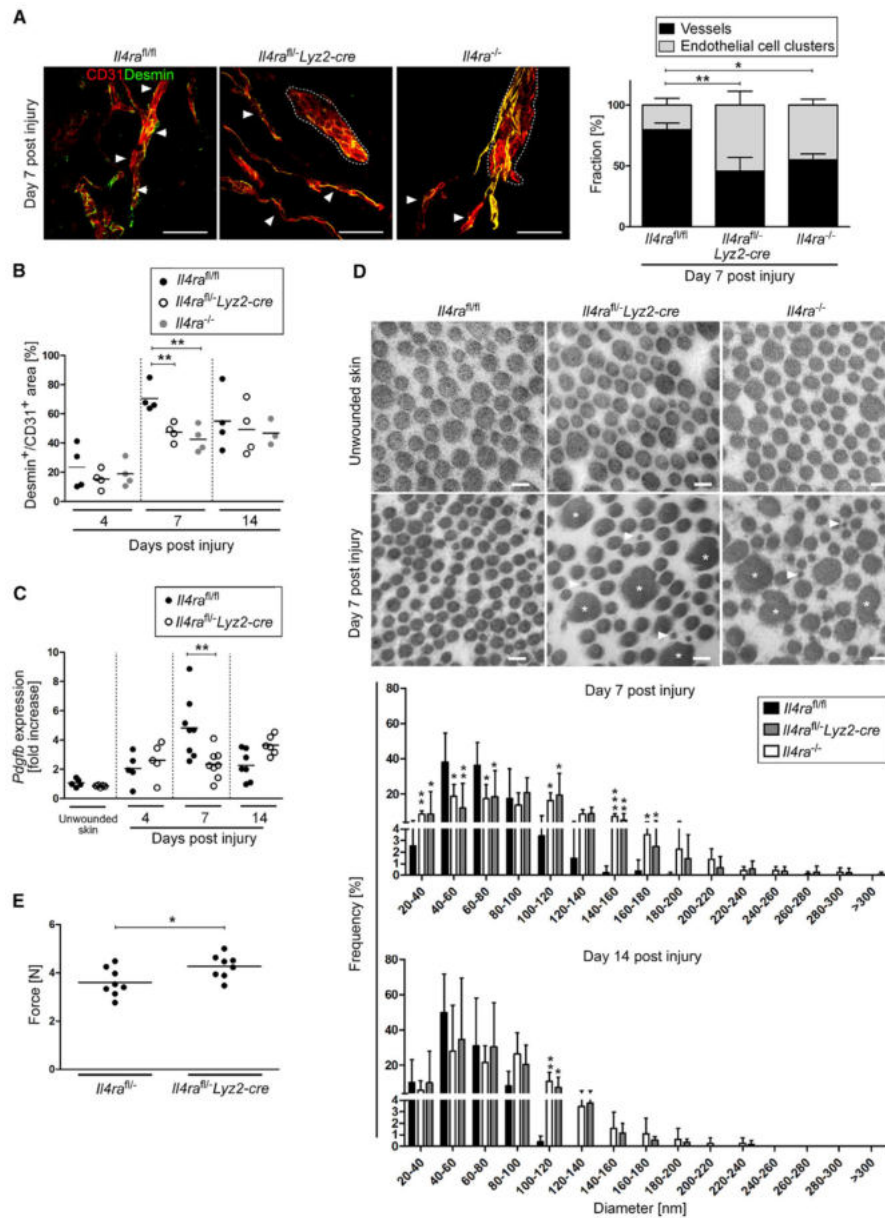


Figure 2. IL-4Ra Signaling in Macrophages Controls Collagen Fibril Formation and Vascular Structures

(A) (left) 3D confocal imaging analysis of IHC double staining for CD31 and Desmin on wound section at 7 dpi; networks of tube-like structures (vessels, indicated by arrow heads) and aggregates of endothelial cells (clusters, outlined by dotted lines) in genotypes are shown as indicated. Scale bar represents 50 μ m. (right) Percentage of CD31⁺ structures organized in vessels or clusters within granulation tissue; n = 3 wounds of 3 mice per genotype.

(B) Quantification of Desmin⁺/CD31⁺ area at indicated dpi.

(C) qRT-PCR gene-expression analysis of *Pdgfb* in wound tissue in relation to unwounded skin.

(D) Ultrastructural analysis of collagen fibrils in unwounded skin and wound granulation tissue at 7 dpi, scale bar represents 100 nm; quantification of fibril diameter at 7 and 14 dpi (n = 1,600 collagen fibrils in 5–7 wounds of 4–7 mice per time point).

(E) Tensile strength test of wound tissue at 16 dpi. Presented is the force required to rupture the scar tissue. Each dot represents one wound; data are expressed as the mean and, where indicated, with \pm SD; *p < 0.05; **p < 0.01; ***p < 0.001.

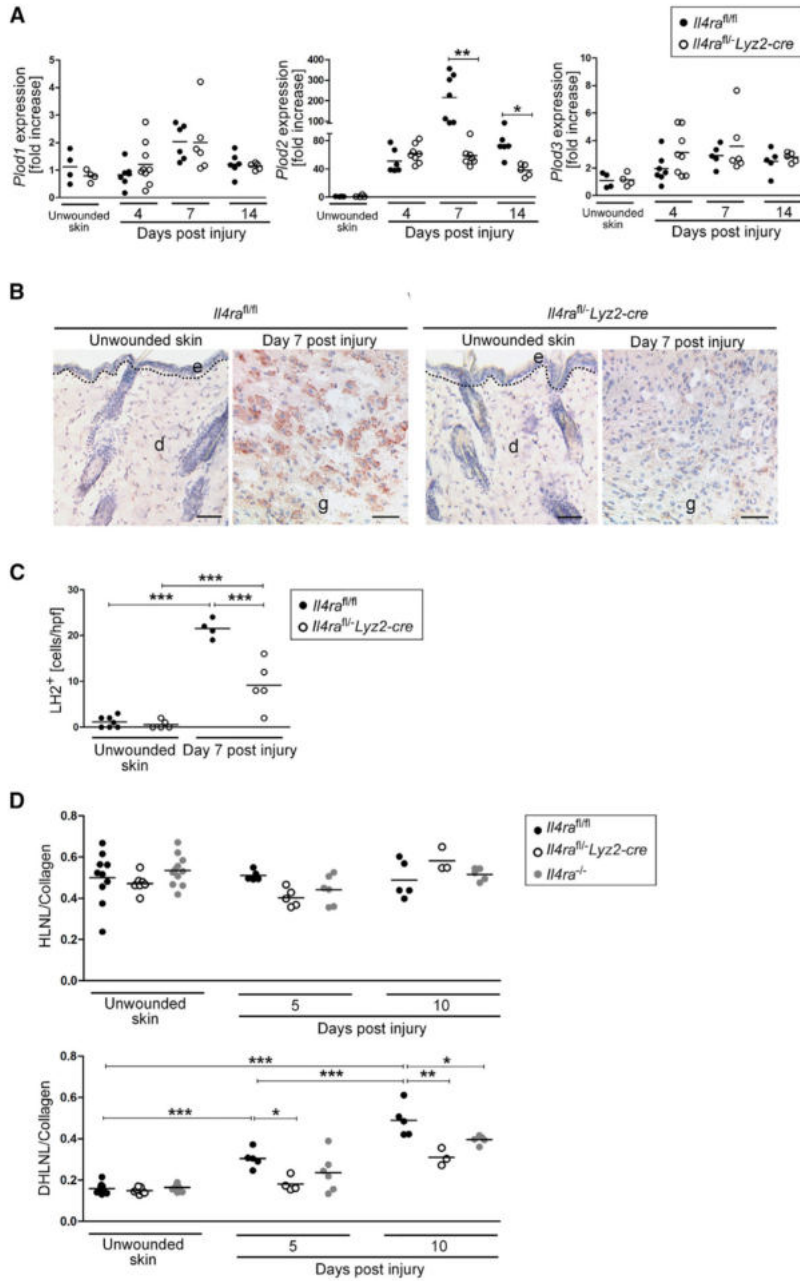


Figure 3. IL-4R α Signaling in Macrophages Directs *Plod2* Expression and Collagen Cross-Links in Wounds

(A) qRT-PCR gene-expression analysis of collagen modifying enzymes in wound tissue in relation to unwounded skin.

(B) IHC staining for LH2 (brown). Scale bar indicates 50 μ m.

(C) Quantification of LH2⁺ cells per high power field (hpf) in granulation tissue at 7 dpi and unwounded skin. d, dermis; e, epidermis; g, granulation tissue. The dashed line indicates the junction between the epidermis and dermis.

(D) Analysis of collagen cross-link formation in unwounded skin and wound tissue. Each dot represents one wound; data are expressed as the mean. * $p < 0.05$; ** $p < 0.01$; *** $p < 0.001$.

Author Manuscript

Author Manuscript

Author Manuscript

Author Manuscript

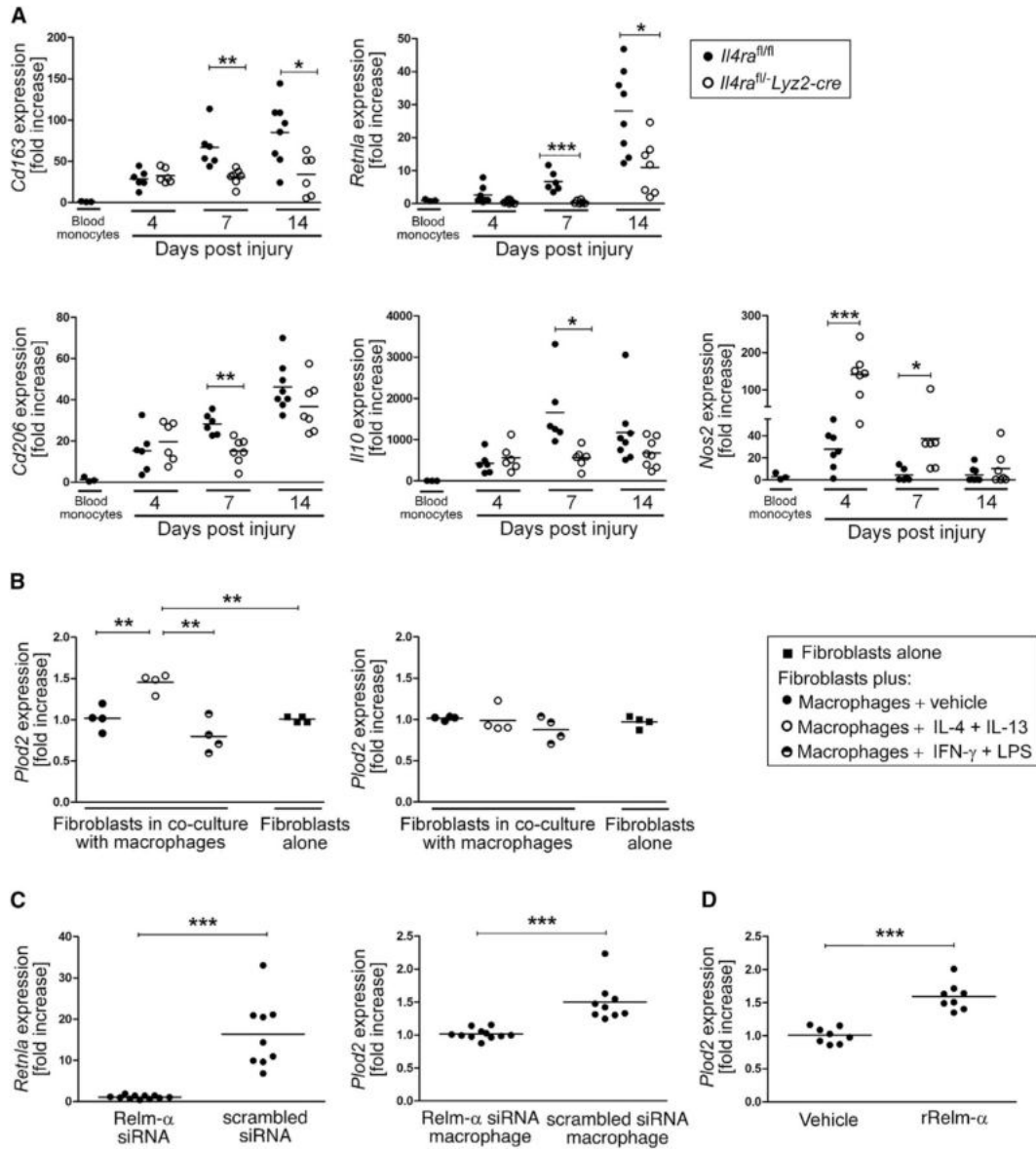


Figure 4. Relm- α Released by IL-4Ra-Regulated Alternatively Activated Macrophages Controls *Plod2* Expression in Fibroblasts

(A) qRT-PCR gene-expression analysis of flow cytometry-sorted CD11b⁺F4/80⁺ wound macrophages in comparison to SSC^{low}CD11b⁺ blood monocytes during healing; each dot represents one wound.

(B) (left) qRT-PCR analysis of primary dermal fibroblasts (*Il4ra*^{-/-}) co-cultured with differently activated bone-marrow-derived macrophages (*Il4ra*^{fl/fl}); (right) qRT-PCR analysis of primary dermal fibroblasts (*Il4ra*^{fl/fl}) co-cultured with differently activated bone-marrow-derived macrophages (*Il4ra*^{-/-}).

(C) (left) qRT-PCR analysis of bone-marrow-derived macrophages transfected with siRNA targeting or non-targeting (scrambled siRNA) *Retnla* mRNA; (right) qRT-PCR analysis of

fibroblasts after co-culture with bone-marrow-derived macrophages transfected with siRNA targeting or non-targeting (scrambled siRNA) *Retnla* mRNA.

(D) qRT-PCR of fibroblasts stimulated with rRelm- α (1 $\mu\text{g}/\text{mL}$).

(B–D) Each dot represents one independent experiment, and each experiment was performed in triplicates. Data are expressed as mean. * $p < 0.05$; ** $p < 0.01$; *** $p < 0.001$.

This figure is supported by Figure S4.

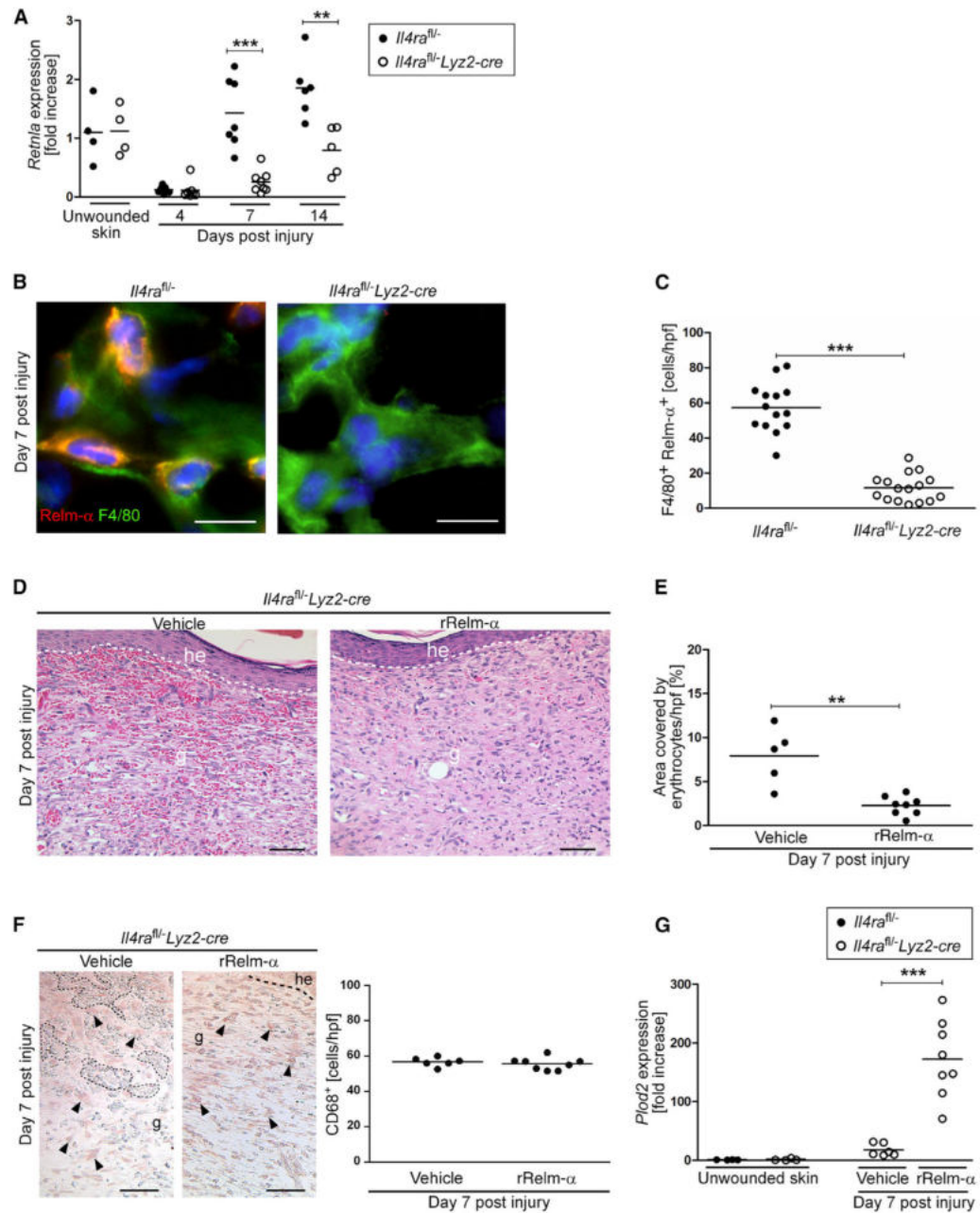


Figure 5. Local rRelm- α Administration Rescues Wound-Healing Pathology and *Plod2* Expression in *Il4ra^{fl/-}Lyz2-cre*

(A) qRT-PCR analysis of *Retnla* in wound tissue normalized to unwounded skin.

(B) F4/80 and Relm- α double immunostaining of wound section at 7 dpi. Scale bar represents 10 μ m.

(C) Quantification of F4/80⁺Relm- α ⁺ cells at 7 dpi.

(D–G) Wounds in *Il4ra^{fl/-}Lyz2-cre* mice repeatedly injected with rRelm- α or vehicle, harvested at 7 dpi. (D) Representative H&E sections (scale bar represents 50 μ m), (E)

quantification of hemorrhages, (F) staining for CD68⁺ (macrophages are indicated by arrow heads; dotted lines outline hemorrhages; the dashed line indicates the junction between the

epidermis and dermis; scale bar represents 50 μm) and quantification, (G) qRT-PCR analysis of *Plod2* in wound tissue normalized to unwounded skin. he, hyperproliferative epidermis; g, granulation tissue. Each dot represents one wound and data are expressed as the mean. **p < 0.01; ***p < 0.001.

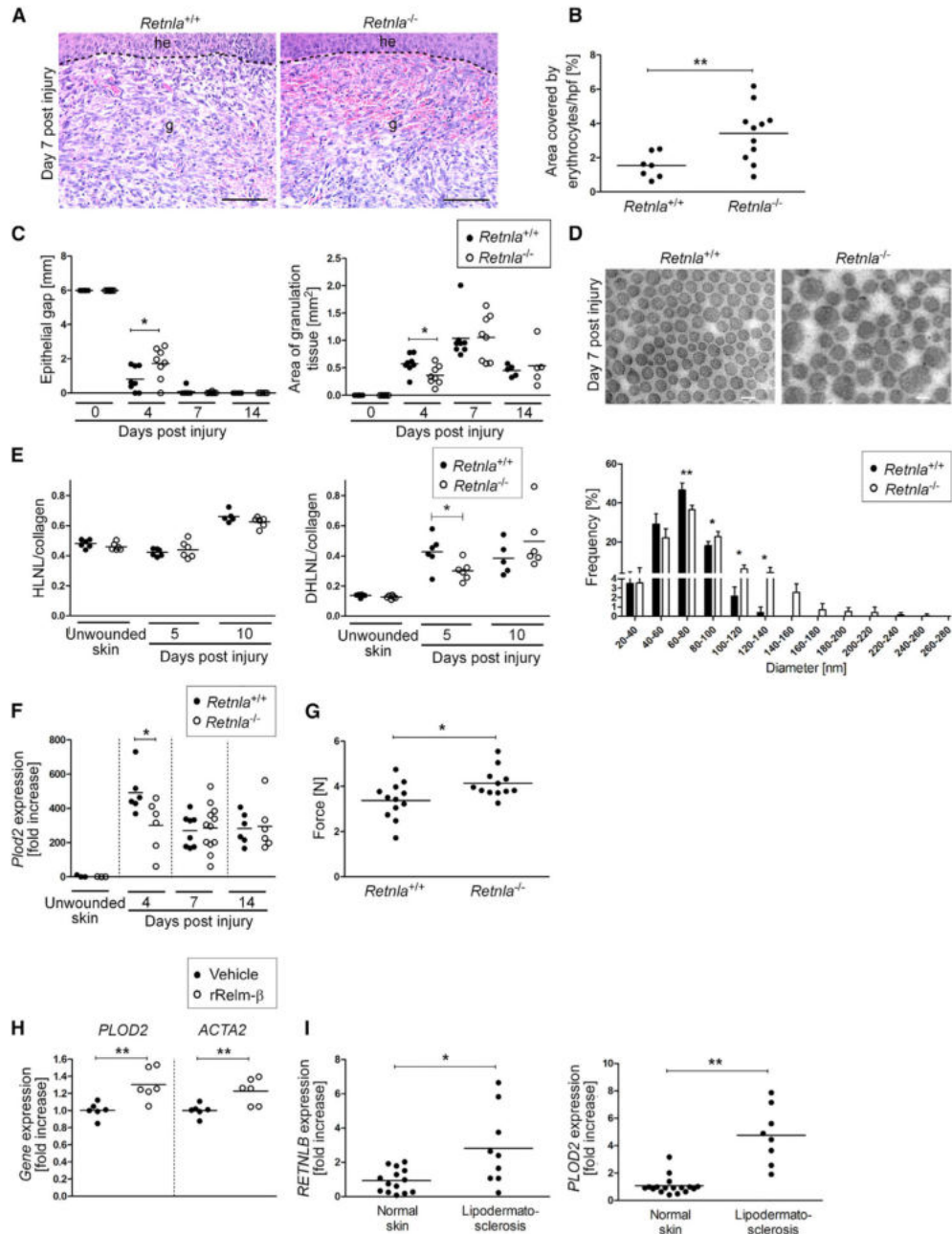


Figure 6. *Retnla*^{-/-} Mice Show Wound-Healing Pathologies Similar to Those of *Il4ra*^{fl/-}*Lyz2-cre* Mice

(A) Representative H&E staining of granulation tissue. Scale bar represents 100 μm.
 (B) Quantification of hemorrhages in the granulation tissue at 7 dpi.
 (C) Morphometric analysis of wound-closure kinetics, quantification of granulation tissue (4 and 7 dpi) and scar (14 dpi) formation at indicated dpi (n = 5–8 wounds of 3–4 mice per genotype and time point).
 (D) Ultrastructural analysis of collagen fibrils in unwounded skin and wound granulation tissue at 7 dpi (scale bar represents 100 nm); quantification of fibril diameter at 7 dpi (n =

1,300 collagen fibrils in 3–5 wounds of 3–4 mice per genotype); data are expressed as the mean \pm SD.

(E) Analysis of collagen cross-link formation in unwounded skin and wound tissue.

(F) qRT-PCR analysis of *Plod2* expression in wound tissue normalized to unwounded skin.

(G) Tensile strength test of wound tissue at 16 dpi; the force required to rupture the scar tissue is presented.

(H) qRT-PCR analysis of human skin fibroblasts stimulated with vehicle or human rRelm- β as indicated (n = 6 per condition, obtained from fibroblasts of two different donors).

(I) qRT-PCR analysis of *RETNLB* and *PLOD2* expression in skin from patients with lipodermatosclerosis in comparison to expression in normal skin; each dot represents one donor. g, granulation tissue; he, hyperproliferative epithelium; each dot represents one wound. Data are expressed as the mean. *p < 0.05; **p < 0.01. This figure is supported by Figure S5.